

Use of Motion Sensors for Autonomous Monitoring of Hydraulic Environments

Nihal Kularatna, Senior Member

Dept of Engineering, The University of Waikato
Private Bag 3105, Hamilton 3240, New Zealand
Email: nihalkul@waikato.ac.nz

Abstract— Low cost, miniaturized, Commercial-Off-The-Shelf (COTS) motion sensors, collectively with processors, an energy source and other electronic circuitry can be packaged into very small volumes for autonomous operation. If such a system operates over short periods of time, or data acquisitions occur at a very low frequency, processor resources should be sufficient to manage offsets and errors. The paper analyzes a typical set of COTS accelerometers and gyroscopes, to indicate how best these can be used in hydraulic environments. Application examples such as river bed sediment monitoring, milk vat monitor etc are briefly discussed, with application oriented design approaches. Minimizing the power consumption to introduce a novel, rechargeable power supply design is briefly outlined.

I. INTRODUCTION

Low cost, miniaturized, Commercial-off-the-Shelf (COTS) motion sensors such as accelerometers and gyroscopes are now commonly available. These together with an energy source and other electronics can be packaged into miniaturised units which can operate autonomously to trace its trajectory or the motion related parameters. Applications are in liquid environments such as river beds [1, 2], milk vat or any other liquid subject to motion with or without turbulence. The “Smart Sediment Particle”, which is capable of tracking its’ own trajectory, has been developed under these principles [2]. If these autonomous, robot-like systems operate for short periods of time, varying from few minutes to few hours or large sampling intervals are used, the processor resources would be sufficient to manage typical issues such as the offset errors etc.

II APPLICATIONS

A. Implementation examples

The “Smart Sediment Particle” is an artificial pebble, which equipped with accelerometers and gyroscopes together with a PIC processor used to track its self trajectory, in a riverbed environment[2]. Although sand and gravel particles in a riverbed are generally stationary, changes in river flow and turbulent currents cause these particles to move. The

Dulsha K. Abeywardana, Student Member

Dept of Electrical and Computer Engineering
The University of Auckland New Zealand
Email: dulsha@hotmail.com

initial pick-up motion, also known as ‘entrainment’ of these particles can be analyzed with the aid of this sensor embedded artificial pebble. Figure 1 illustrates the implemented “Smart Sediment Particle.” The “Smart Sediment Particle” utilizes two ADXL202 dual axis accelerometers and three ADXRS150 gyroscopes. These measurements are read into the micro-controller over the ADC channels and stored away in an external memory for later retrieval. The data is later downloaded onto a PC for processing with the aid of MATLAB. The unit is designed to operate for short periods of time to avoid cumulative errors.

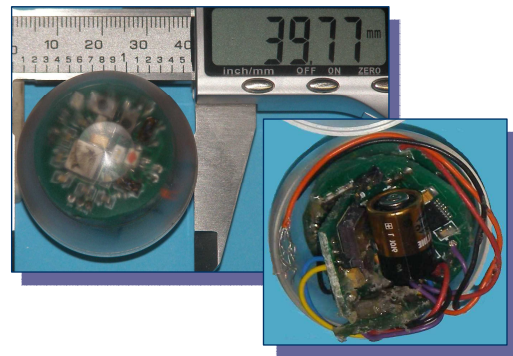


Figure 1. Implemented Smart Sediment Particle

Another possible application of the technique is to monitor the conditions in a milk vat for the parameters of temperature and the agitator operation.

B. Operational Technique

Basic concepts of an Inertial Navigation System (INS) [1] have been used to process the sensor data. In INSs the exact location of the object concerned can be determined with respect to a known initial location. The exact location of the object in three dimensional space is calculated by integrating the accelerations and rotations about the three axes. Accelerometers are placed to measure the acceleration about each orthogonal axis in 3D space while three gyroscopes measure the angular acceleration about each axis. These sensors are placed to form a reference frame consisting of three orthogonal axes, known as the “Body Frame.” Forces acting on the particle are measured with respect to this Body Frame, which is in constant motion. Therefore in order to obtain a reading for each measurement

with respect to a stationary frame an axis conversion technique needs to be used. There are several methods of performing this coordinate transformation [3] such as Euler Angle, Direction Cosine and Quaternion. The Euler Angle method [4] was chosen based on its simplicity and for the ease of processing. The Euler Angle performs the transformation to reference frame by taking three successive rotations about three orthogonal axes in turn [3]. The angular rotations about z, y and x axes are taken as ψ , θ and ϕ . Figure 2 depicts the alignment of the orthogonal axes, and the positive rotation direction about each axis.

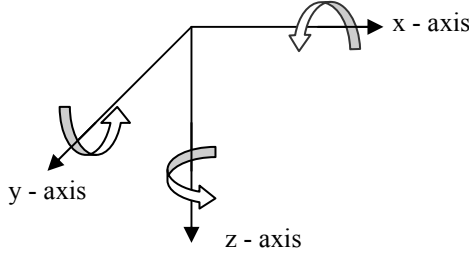


Figure 2. Orthogonal Axes and Positive Rotation Direction about Each Axis

With positive rotations about each axis three cosine matrices can be obtained as C_1 , C_2 and C_3 . Rotation about z axis produces the matrix C_1 ,

$$C_1 = \begin{bmatrix} \cos \psi & \sin \psi & 0 \\ -\sin \psi & \cos \psi & 0 \\ 0 & 0 & 1 \end{bmatrix}$$

This changes the orientation of the entire body frame. The rotation about the new y axis produces C_2 .

$$C_2 = \begin{bmatrix} \cos \theta & 0 & -\sin \theta \\ 0 & 1 & 0 \\ \sin \theta & \cos \theta & 0 \end{bmatrix}$$

The rotation about the new x axis produces C_3 .

$$C_3 = \begin{bmatrix} 1 & 0 & 0 \\ 0 & \cos \phi & \sin \phi \\ 0 & -\sin \phi & \cos \phi \end{bmatrix}$$

The transformation from reference to body frame is given by the product of these three matrices which is the rotation matrix,

$$C_b^n = C_3 \cdot C_2 \cdot C_1$$

The inverse of this transformation, the body to reference frame transformation is given by the direction cosine matrix,

$$C_b^n = C_n^{bT} = C_1^T \cdot C_2^T \cdot C_3^T$$

$$C_b^n = \begin{bmatrix} \cos \psi & -\sin \psi & 0 \\ \sin \psi & \cos \psi & 0 \\ 0 & 0 & 1 \end{bmatrix} \begin{bmatrix} \cos \theta & 0 & \sin \theta \\ 0 & 1 & 0 \\ -\sin \theta & 0 & \cos \theta \end{bmatrix} \begin{bmatrix} 1 & 0 & 0 \\ 0 & \cos \phi & -\sin \phi \\ 0 & \sin \phi & \cos \phi \end{bmatrix}$$

$$C_b^n = \begin{bmatrix} \cos \theta \cos \psi & -\cos \phi \sin \psi + \sin \phi \sin \theta \cos \psi & \sin \phi \sin \psi + \cos \phi \sin \theta \cos \psi \\ \cos \theta \sin \psi & \cos \phi \cos \psi + \sin \phi \sin \theta \sin \psi & -\sin \phi \cos \psi + \cos \phi \sin \theta \sin \psi \\ -\sin \theta & \sin \phi \cos \theta & \cos \phi \cos \theta \end{bmatrix}$$

It can be assumed that for small angles $\sin x \rightarrow x$ and $\cos x \rightarrow 1$. Considering the relatively fast sampling and slow angular rotations this assumption can be used, and by ignoring products of angles which become infinitesimally small, the above equation can be simplified to a skew symmetric form as,

$$C_b^n = \begin{bmatrix} 1 & -\psi & \theta \\ \psi & 1 & -\phi \\ -\theta & \phi & 1 \end{bmatrix}$$

Multiplying the body frame by the transpose of the rotation matrix produces the conversion of any vector from the body frame to the reference frame.

$$r^n = C_b^n \cdot r^b$$

If Commercial Off-The-Shelf (COTS) accelerometers and gyroscopes are used for this system, r^b can be indicated as below. A_{x-b} , A_{y-b} and A_{z-b} are the accelerations of the body frame along the corresponding axes.

$$C_b^n = \begin{bmatrix} A_{x-b} \\ A_{y-b} \\ A_{z-b} \end{bmatrix}$$

This gives a simplified expression for r^n as,

$$r^n = \begin{bmatrix} 1 & -\psi & \theta \\ \psi & 1 & -\phi \\ -\theta & \phi & 1 \end{bmatrix} \begin{bmatrix} A_{x-b} \\ A_{y-b} \\ A_{z-b} \end{bmatrix}$$

If ω_z , ω_y and ω_x are gyrations about each axis respectively,

$$\psi = \int \omega_z dt \quad \theta = \int \omega_y dt \quad \phi = \int \omega_x dt$$

Using these basic relationships the accelerations along each axis, with respect to a known reference frame can be calculated. Currently this processing is done offline, in MATLAB. However with a powerful processor subsystem it can be moved on to the processor subsystem itself.

C. Performance

A typical set of sensor readings provides the acceleration of the particle along each axis in 3D. Figure 3 outlines the acceleration of the particle when placed on a shake table with a known acceleration. The shake table's acceleration is plotted together with the acceleration of the pebble as measured by the embedded sensors. However, the data extracted from the pebble, displayed a small degree of offset and errors. These errors accumulate over time and are multiplied once the acceleration data is double integrated to retrieve the distance. Therefore measures to reduce these errors are vital, to achieve a realistic and accurate reading.

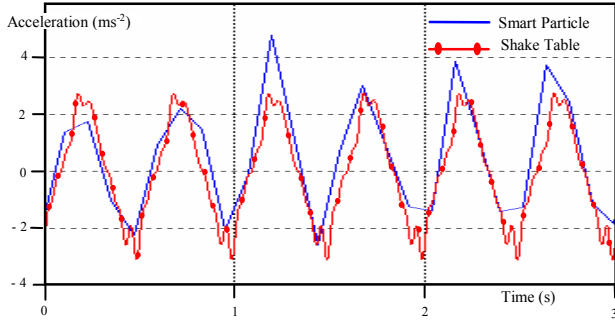


Figure 3. One Dimensional Acceleration of Smart Particle and Shake Table

D. Error Sources

Data conversion devices such as Analog-to-Digital-Converters (ADC) interface between continuous time signals and their discrete time digital equivalent [5]. For an ADC with n -bit resolution with a full scale of signal value between 0 and V_{FS} , 2^n is the resolution limit. The quantizing interval q can be calculated as,

$$q = \frac{V_{FS}}{(2^n - 1)}$$

If an input signal falls between the V_j th level range of $\pm q/2$ a quantization error of ϵ is created, which may range up to $\pm q/2$. Assuming the conventional probability density function of noise, which is uniformly distributed along the interval $\pm q/2$, the equivalent rms quantization error can be calculated as,

$$\text{Quantization Error} = \left(\frac{1}{q} \int_{-q/2}^{q/2} \epsilon \cdot d\epsilon \right)^{1/2} = \frac{q}{2\sqrt{3}}$$

When using a microcontroller with a 10-bit ADC and a reference voltage of 5V, q works out to be 0.0049V. This creates an rms quantization error of 0.0014V. Although this is an insignificant value when considered individually, the cumulative error created over a period of time would lead to a significant error.

Choosing the correct sampling frequency is vital to avoid undesired amplitude errors [5, 7]. The time domain amplitude error between the sampled signal and the real signal is directly proportional to the ratio between signal amplitude and range of the ADC. The amplitude error ϵ can be approximated as,

$$\epsilon = \frac{\sqrt{2} \pi V_{S-pk} BW}{\sqrt{5} f_s V_{FS-pk}}$$

V_{S-pk} is the peak value of the input signal, BW is the bandwidth of the signal, f_s is the sampling frequency and V_{FS-pk} is the full scale ADC range. Therefore it is apparent that increasing both the sampling frequency and the ADC range can reduce the amplitude error.

Apart from the data conversion errors mentioned other error sources contribute in distorting the sensor data further.

The estimated direction cosine matrix, \hat{C}_b^n can be written in terms of the true direction cosine matrix C_b^n as [3],

$$\hat{C}_b^n = B C_b^n$$

where B is the transformation from the true reference axes to the true reference axes. For small angles of misalignment B is approximated as,

$$B = [I - \Psi]$$

with I being a 3x3 identity matrix and Ψ is given by,

$$\Psi = \begin{bmatrix} 0 & -\delta\gamma & \delta\beta \\ \delta\gamma & 0 & -\delta\alpha \\ -\delta\beta & \delta\alpha & 0 \end{bmatrix}$$

$\delta\alpha$ and $\delta\beta$ are attitude errors with respect to the vertical and the level or tilt errors. $\delta\gamma$ is the error about the vertical, the heading or azimuth error. Apart from these errors, the assumption the $\sin x \rightarrow x$ and $\cos x \rightarrow 1$ also leads to a errors in the calculations, in the long run. Therefore it is evident that the direction cosine matrix, which is relied upon to perform the axis transformation is not completely accurate and thus can create a cumulative error in the long run.

Velocity and position errors in an INS are mainly due to attitude errors as discussed previously [3]. Inaccuracies in measurements of the specific force provided by the accelerometers also contribute to errors in velocity and position calculation. Errors in the Coriolis terms, differences in local gravity vector and incorrect assumptions about the shape of the earth although negligible, also make a difference in calculations. Out of these for a short duration and short range motion parameter estimation, last three error sources could be neglected.

Another main error source is the basic offset and gain errors in the MEMS and associated signal conditioning circuits. The ADXL202 has noise characteristics of white Gaussian noise, contributing equally at all frequencies [6]. The noise is proportional to the square root of the bandwidth of the accelerometer. Reducing the bandwidth can reduce the noise and improve the resolution. The manufacturers recommend that the bandwidth should be limited to the lowest frequency required by the application to maximize the resolution and the dynamic range of the sensor. Other factors such as variations in temperature, supply current and voltage etc., also affect the resolution of these sensors.

II. USE OF LOW COST MEM SENSORS

Literature indicates that the devices such as ADXL and ADXRS series of COTS are usable as strap-down Inertial Measurement Units (IMU) in complex projectiles like ammunition etc [7]. These devices can withstand shocks ranging from 5-500g's and encourages the use of these for simpler applications in liquid environments discussed here. These devices are used in detecting static and dynamic

activities also in addition to their heavy commercial usage in automotive airbags and consumer electronics etc [8].

III. ERROR COMPENSATION

Some simple techniques to overcome errors are, reducing the bandwidth, increasing the sampling frequency and increasing the reference voltage for ADCs. These are discussed in [5,9].

By mounting the system on a level table with each sensitive axis pointing up and down alternatively, estimates can be made on the accelerometer biases, scale factor errors and sensitive axis misalignments [3]. With a sufficient number of this six position tests, a single value can be calculated to model each error and offset, which can be integrated as a correction factor when the data is being processed.

The static rate test can be conducted for different orientations of the unit, to estimate fixed and g-dependent biases for each gyroscope [3]. These fixed biases can easily be appended to the gyroscope readings to improve their accuracy. The g-dependent biases will need to be modelled into a formula, with the aid of measurement statistics and then integrated into the calculations to minimize errors. To derive estimates of gyroscope measurements a precision multi-position test table can be used [3]. By rotating the unit through known angles and then obtaining the calculated angle using the sensor measurements, these errors can be estimated. Again an error model can be generated and modelled to correct the measurement as desired.

II FUTURE DEVELOPMENTS

A. Power Supply Design

The power supply design is currently limited to a 6V battery, a charge pump and a voltage regulator. The charge pump keeps the supply voltage at $5V \pm 4\%$, as the battery power diminishes over time. It can take an input voltage ranging between 2.7-5.4V, to produce a regulated 5V output. The circuit operates smoothly, minimizing undesired resolution errors at sensor outputs and A/D conversions. Slight variations in supply voltage would change the reference voltage for sensors and the ADC of microcontroller and thus generating errors.

One of the main issues with this system is the battery life, which is about 15-20 minutes of continuous operation. Work is being carried out to design a wireless, rechargeable power supply using Inductive Power Transfer (IPT) technology. The unit will be recharged when it's not operational. A miniature secondary pickup within the particle would inductively collect energy from the primary IPT power supply and store it within a combination of rechargeable cells and super capacitors. When the unit is operational the energy stored within will be discharged economically. The proposed design is outlined in Figure 4.

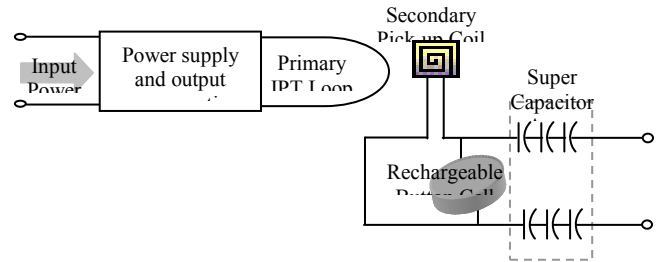


Figure 4. Basic Setup of Proposed Power Supply Design

B. Minimizing Power Consumption

With the new power supply design the next key issue to be addressed is the power consumption. One of the main design changes proposed, is to replace the existing microcontroller with a low power microcontroller. Work is now underway to adapt a Silicon Labs microcontroller which operates with a supply voltage as low as 0.9V. With a supply range between 0.9-1.8, 10-bit ADC supporting up to 23 external inputs it would be ideal for this application. Moreover the miniaturized package is an added advantage for small PCB real estate. The circuit design is also to be optimized further to minimize the power consumption and better voltage regulation.

CONCLUSIONS

In conclusion, use of COTS type MEMS with suitable other electronic subsystems can be implemented to monitor the physical and motion parameters in liquid environments. The smart sediment particle is one example and milk vat monitor is another. Studying common error sources affecting the MEMS and data conversion devices, certain error compensation techniques can be proposed. Many other applications can be developed under the same basic principles, for applications where sensor units are needed to monitor environments without disturbing their natural processes.

REFERENCES

- [1] N. Kularatna, et al, "Implementation aspects and offline digital signal processing of a smart pebble for river bed sediment transport monitoring," Proc. of IEEE Sensors 2006, Daegu, Korea, Oct 2006.
- [2] N. Kularatna, & B. Melville, "Experiences and design challenges in developing a smart sediment particle for monitoring sediment transport in river beds," Proc. of CIM'07, Malaysia, 2007, pp 778-784.
- [3] D. H. Titerton and J. L. Weston, "Strapdown inertial navigation technology," IEE, 1997.
- [4] R. Pio, "Euler angle transformations," IEEE Transactions on Automatic Control, Volume 11, Issue 4, Oct 1966, pp. 707 - 715.
- [5] P. H. Garret, "High performance instrumentation and automation," CRC Press and Taylor & Francis Group, 2005.
- [6] Analog Devices, Datasheet -ADXL202/ADXL210, Revision B, 2004.
- [7] Davis, B.S, "Using low-cost MEMS accelerometers and gyroscopes as strapdown IMUs on rolling projectiles," Position Location and Navigation Symposium, IEEE 1998, April 1998 pp. 594 - 601
- [8] Veltink, P.H et al, "Detection of static and dynamic activities using uniaxial accelerometers", IEEE Trans. on Rehabilitation Engineering, Vol 4, No 4, Dec 1996, pp 375-385.
- [9] Analog Devices Inc., AN-767 Application Note, 2005.